

Electronic phase transitions in the half-filled ionic Hubbard model

L. Craco,¹ P. Lombardo,² R. Hayn,² G. I. Japaridze,³ and E. Müller-Hartmann⁴

¹Max-Planck-Institut für Chemische Physik fester Stoffe, 01187 Dresden, Germany

²Laboratoire Matériaux et Microélectronique de Provence associé au Centre National de la Recherche Scientifique,

UMR 6137, Faculté Saint-Jerôme, 13397 Marseille Cedex 20, France

³Andronikashvili Institute of Physics, Tamarashvili 6, 0177 Tbilisi, Georgia

⁴Institut für Theoretische Physik, Universität zu Köln, Zùlpicher Strasse 77, 50937 Köln, Germany

(Received 7 June 2007; revised manuscript received 21 March 2008; published 25 August 2008)

A detailed study of electronic phase transitions in the ionic Hubbard model at half filling is presented. Within the dynamical mean field approximation a series of transitions from the band insulator via a metallic state to a Mott–Hubbard insulating phase is found at intermediate values of the one-body potential Δ with increasing the Coulomb interaction U . We obtain a critical region in which the metallic phase disappears and a coexistence phase between the band and the Mott insulating state sets in. Our results are consistent with those obtained at low dimensions, thus they provide a concrete description for the charge degrees of freedom of the ionic Hubbard model.

DOI: [10.1103/PhysRevB.78.075121](https://doi.org/10.1103/PhysRevB.78.075121)

PACS number(s): 71.10.Hf

One important problem in the field of electronic structure theory is the understanding of the Mott metal-insulator transition (MIT).^{1,2} Many details have already been clarified using the canonical model for this transition—the one-band Hubbard model. At half filling (i.e., having in average one electron at each lattice site) this transition from the metallic to the Mott–Hubbard insulating (MI) phase occurs with increasing the on-site repulsion U . Great progress in understanding the MIT in Hubbard-type models has been achieved in the last decade with the development of the dynamical mean field theory (DMFT). Although many aspects of the coherent (Fermi liquid) metallic phase and the incoherent MI phase are now quite well understood, other questions remain open, especially the relationship between the MI regime and band insulators (BI), where one sub-band is almost completely filled by two electrons such that an excitation gap is formed.

To study the interplay between band and Mott–Hubbard insulators, various extended versions of the one-band Hubbard model have been proposed. It is remarkable that different models show separate kinds of behavior. Some of them have a crossover from the BI to the MI regime,³ whereas others have clear transition points with a metallic phase in between.⁴ A widely studied model for the second class is the ionic Hubbard model (IHM).^{5–7} In the one-dimensional (1D) IHM, however, a ferroelectric (or bond-ordered) phase is realized which separates BI and MI, and the metallic phase shrinks to only one point.^{10,11} Already in 1D, a finite metallic region can be recovered by introducing an intrasublattice hopping t' into the IHM.¹² In 2D (Ref. 7) or at larger dimensions⁵ a correlation induced metallic phase was reported between BI and MI, but it is still under debate whether this metallic phase shrinks to a line⁵ or if it ends up at a particular point by increasing the ionicity Δ . In this work we show that the metallic phase disappears at a certain value of Δ above which we found a coexistence region composed of distinct insulating phases.

It might not be very surprising to find quite different behavior in various models at different dimensions. But even if we restrict our attention to the IHM, the phase diagram is

highly disputed. The 2D case was studied by a cluster extension of DMFT (Ref. 7) and by the determinant quantum Monte Carlo method^{6,8} showing different results. The cluster-DMFT study suggests a bond-order phase separating BI and MI regimes, while the stability of the metallic phase was established on a 2D square lattice at finite temperatures.⁶

To clarify the many open questions related to the electronic phase diagram of the IHM, we study this problem here in the limit of high dimensions. In this limit the self-energy is \mathbf{k} -independent and, thus, the dynamical many-body problem can be mapped onto a single-site one. Using basically the same DMFT scheme as Garg *et al.*,⁵ we confirm the existence of the metallic phase for moderate values of U/Δ , but we also find important new features which are different from those reported in this recent work. So, for intermediate values of Δ , we find a continuous BI-to-metal phase transition and a discontinuous one between the metallic and the MI phase with increasing the Coulomb interaction U .

We start our study with the IHM

$$H = -t \sum_{i \in A, j \in B, \sigma} (\hat{c}_{i\sigma}^\dagger \hat{c}_{j\sigma} + \text{H.c.}) + U \sum_i \hat{n}_{i\uparrow} \hat{n}_{i\downarrow} + \Delta \sum_{i \in A} \hat{n}_i - \Delta \sum_{i \in B} \hat{n}_i \quad (1)$$

on a bipartite lattice with two sublattices A and B having different on-site energies $\varepsilon_A = +\Delta$ and $\varepsilon_B = -\Delta$. t is the (inter-sublattice) hopping term and U is the on-site Coulomb repulsion. $\hat{c}_{i\sigma}^\dagger$ (respectively $\hat{c}_{i\sigma}$) denotes the creation (respectively annihilation) operator of an electron at the lattice site i with spin σ and $\hat{n}_{i\sigma}$ is the occupation number operator for electrons with spin σ . We consider an average number of one particle per lattice site, i.e., the half-filled case.

To apply the DMFT scheme to the IHM, we have to solve two (A, B) local problems given by the local one-particle Green's functions G_α . At high dimensions, these local propagators are connected self-consistently by the Dyson equation $G_{0\alpha}^{-1} = G_\alpha^{-1} + \Sigma_\alpha$.⁹ Without loss of generality, in what follows we will perform our calculations using a semielliptic density

of states (DOS)—this type of one-particle DOS is realized on a Bethe lattice with infinite coordination number.

On a bipartite A – B lattice with nearest-neighbor hopping t the single-site Green's functions reads

$$G_{\alpha}(\omega) = \xi_{\bar{\alpha}} \int_{-\infty}^{\infty} d\varepsilon \frac{\rho_0(\varepsilon)}{\xi_A \xi_B - \varepsilon^2}, \quad (2)$$

with $\alpha=A$ ($\bar{\alpha}=B$) and $\xi_{\alpha} = \omega + i0^+ - \varepsilon_{\alpha} + \mu - \Sigma_{\alpha}(\omega)$. After integrating Eq. (2) using the semicircular DOS $\rho_0(\varepsilon) = \sqrt{4t^2 - \varepsilon^2}/(2\pi t^2)$, we obtain two coupled equations $G_{\alpha}(\omega)^{-1} = \xi_{\alpha} - t^2 G_{\bar{\alpha}}(\omega)$ for the IHM on a Bethe lattice. As in Ref. 5, we use the iterated perturbation theory (IPT) (Ref. 13) to calculate the local self-energies $\Sigma_{\alpha}(\omega)$. From a direct comparison between different methods^{9,13–15} it is found for the one-band Hubbard model that the quasi-particle peak (Kondo resonance), the position of the Hubbard bands, the Mott–Hubbard gap, as well as the principal characteristics of the metal-insulator transition in infinite dimensions are all well captured by the IPT solver. Since at each lattice site the band filling is always away from one-half in the IHM (see Fig. 5), it is proper to use the canonical IPT *ansatz*: $\Sigma_{\alpha}(\omega) = \Sigma_{\alpha}^{HF} + A_{\alpha} \Sigma_{\alpha}^{(2)}(\omega) / [1 - B_{\alpha} \Sigma_{\alpha}^{(2)}(\omega)]$ for the correlated problem. Within this *ansatz*, $\Sigma_{\alpha}^{HF} = U n_{\alpha}$ is the first-order Hartree term and $n_{\alpha} = -1/\pi \int_{-\infty}^0 \text{Im} G_{\alpha}(\omega) d\omega$. The coefficients A_{α} and B_{α} are determined by requiring $\Sigma_{\alpha}(\omega)$ to be exact at high frequencies and in the atomic limit. Finally, $\Sigma_{\alpha}^{(2)}(\omega) \equiv \Sigma_{\alpha}^{(2)}(\omega, [\tilde{G}_{0\alpha}(\omega)])$ is the well known second-order diagram for the self-energy.¹³

In our treatment, the host Green's functions $\tilde{G}_{0\alpha}$ required to compute $\Sigma_{\alpha}^{(2)}(\omega)$ self-consistently are written as $\tilde{G}_{0\alpha}^{-1} = \mathcal{G}_{0\alpha}^{-1} + \varepsilon_{\alpha} - \mu$. The energy shift $\varepsilon_{\alpha} - \mu$ introduced here accounts for the correct atomic limit of the IHM at $U \gg \Delta, t$ (see below) as well as the mirror-type particle-hole symmetry between sites A and B . Notice that a similar type of correction is employed in the context of single-site Hubbard model ($\varepsilon_A = \varepsilon_B = 0$), where the energy shift is $-\mu$ ($= -U/2$ at half filling).⁹ In addition, we point out that our energy shift is different from the Hartree correction $-\Sigma_{\alpha}^{HF}$ employed in Ref. 5, and this might be the cause for significant differences between our and their results in the large U limit.

Let us now present our results. In Fig. 1, we show the spectral density for the charge phases of the IHM. In the upper panel, we present our result for the BI phase for $U/t = 0.1$. The full line corresponds to the two-site averaged (or the *total*) DOS, whereas the dotted line is the site resolved B -DOS. As expected the charge gap is small, of the order of Δ . We observe clear Van Hove singularities at the lower band edge at each α -site. With increasing U the band gap is suppressed (by dynamical transfer of spectral weight characteristic of correlated electron systems) and a metallic phase sets in. As can be seen in the dotted line of Fig. 1(b), the B -DOS shows a pseudo gap feature at the Fermi level. This implies that the one-particle DOS in the metallic phase is not pinned to its unperturbed ($U = \Delta = 0$) value.¹⁶ This is understood, because the charge density wave (CDW) regime prevents the Fermi liquid fixed point at any value of the Coulomb interaction. As expected in such cases, the imaginary part of

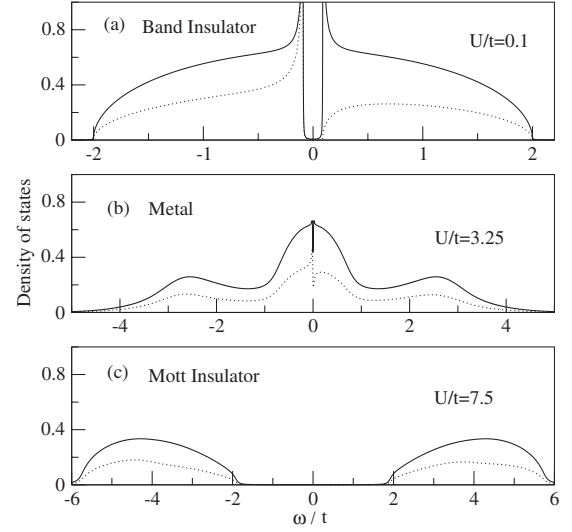


FIG. 1. Total and site-selective (b) DOS for $\Delta = 0.1t$ and various values of U . The parameters are chosen identical to those of Garg *et al.*,⁵ leading to very close results except for the lowest panel (larger gap and V -shape leading edge in the DOS). The imaginary part of the energy is $\delta = 0.0001$. Notice the small difference between the lower and the upper Hubbard band in the site-selective DOS; this results from the softening of the CDW at large U .

$\Sigma_{\alpha}(\omega)$ (not shown) is finite at the Fermi level. The dynamical transfer of spectral weight found in the metallic phase can be traced to a Kondo-type process that leads to strong electron mass enhancement. A similar effect is known to take place in correlated electron systems like the periodic Anderson model⁹ or in some regimes of the disordered Hubbard model.¹⁷ By further increasing U , the Mott–Hubbard insulator with a gap of the order of $U - W$ (W is the bandwidth) sets in as the third phase of the IHM.

Having chosen exactly the same parameters as in Ref. 5 (and basically the same method of solution), we find very similar results for the upper two panels, but substantial differences for the results in the large U regime are observed. In particular, the Van Hove structures found in Ref. 5 near the Fermi energy broaden and shift to high energies for $U = 7.5t$. There is an appreciable modification of the whole line shape. Within our self-consistent scheme the Hubbard bands centered at $\omega \approx \pm 4t$ are in very good agreement with those found for the one-band Hubbard model. Clearly, our results for $U = 7.5t$ are more plausible than those obtained in Ref. 5. Moreover, it is understood that in the large U limit the staggered charge density is small (see results of Fig. 5), forcing one to recover to a good extent the physics of the regular Hubbard model. This is exactly what is shown in the lower panel of Fig. 1.

To characterize the correlated nature of the various phase transitions and the stability of the metallic phase, we show in Fig. 2 the obtained charge gap as a function of U . The charge gap can be used as an order parameter of the BI phase and tends to zero at the BI-metal transition point. Alternatively, we can use the DOS at the Fermi level $\rho(0)$ as an order parameter of the metallic phase (see Fig. 3). To prove the existence of a phase transition and to determine the transition point we have to investigate the scaling behavior of $\rho(0)$

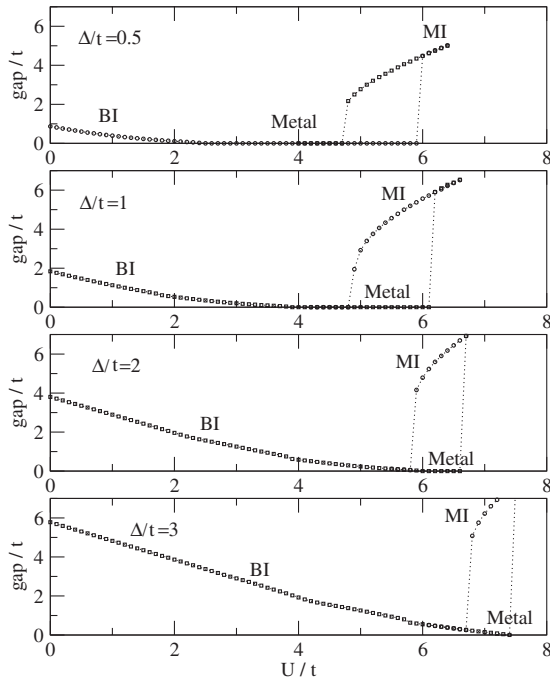


FIG. 2. Charge gap of the IHM as function of U for various values of Δ . The imaginary part of the energy is $\delta=0.0001$. The coexistence region between metal and Mott insulator (MI) is reminiscent of DMFT for the pure Hubbard model.⁹ At large values of Δ the metallic phase shrinks and, we obtain a coexistence region for the band (BI) and Mott insulators.

when the imaginary part of the energy δ for the retarded Green's function tends to zero. In the case of a finite gap, $\rho(0)$ depends linearly on δ which is well observed in Fig. 3. On the other hand, in the metallic phase, we observe a finite $\rho(0)$. In such a way, the phase transition line can be determined.

As can be seen in Fig. 2, the width of the metallic phase shrinks with increasing Δ , until it disappears at a critical value. For $\Delta \leq 1.9t$, we find a continuous transition from the BI to a unique metallic phase with increasing U . In contrast

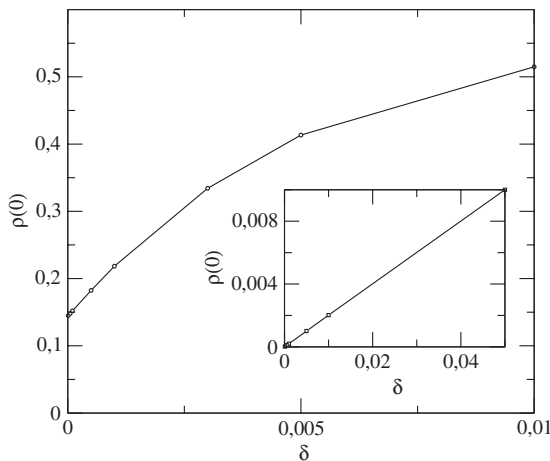


FIG. 3. Density of states at the Fermi level $\rho(0)$ as a function of the imaginary part of the energy δ for $U=3.2t$ and $\Delta=0.1t$ (metallic region) and in the BI case ($U=t$, $\Delta=2t$, inset).

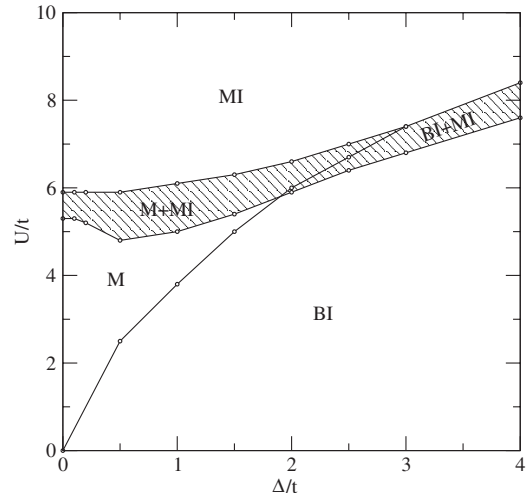


FIG. 4. Phase diagram of the IHM obtained by single-site DMFT. The dashed area corresponds to the coexistence region between metal (M) and Mott insulator (MI) or between band insulator (BI) and Mott insulator, respectively.

to the BI-to-metal transition, the transition from the metallic phase to the Mott insulator phase is of the first order. The latter transition in the IHM is completely identical to the corresponding transition in the ordinary Hubbard model. Across the metal-to-MI transition line we observe a coexistence region consisting of two distinct (numerical) solutions, which is accompanied by a hysteresis loop characteristic of a first-order MIT.⁹ In agreement with previous theoretical studies,^{5,7} the width of the coexistence region decreases with increasing ionicity (Δ). For larger values of Δ , the metallic phase disappears and a coexistence region between BI and MI is found.

The obtained phase diagram for the IHM on a Bethe lattice is shown in Fig. 4. It differs considerably from those found and/or recently proposed for the IHM on a usual bipartite lattice in two or at high dimensions.⁵⁻⁸ In contrast to previous single-site DMFT results,⁵ the metallic phase is now considerably widened. The first-order metal-to-MI and BI-to-MI phase transitions resemble the coexistence region found by Kancharla *et al.* in 2D.⁷ In addition, our window for the metallic region at moderate values of Δ is similar to the determinant quantum Monte Carlo study also in 2D,^{6,8} indicating common similarities between the physics at low and high dimensions for the IHM. To further illustrate the underlying features in the coexistence region and the first-order phase transitions, we show in Fig. 5 the staggered charge density $n_B - n_A$ as a function of U . As one can see, the curves are continuous at the transition point between the BI and the metallic phase. However, the staggered charge density jumps at the transition toward the MI phase.

The possibility of having different types of first-order phase transitions in the IHM (see Fig. 4) is one relevant aspect of our work. Furthermore, our results show that the coexistence region is not necessarily connected with the bond-order phase recently found with cluster-DMFT for the 2D-IHM.⁷ We find that a first-order transition between metal and MI (or between BI and MI) exists not only in 2D but also at high dimensions. Thus, the first-order MIT of the

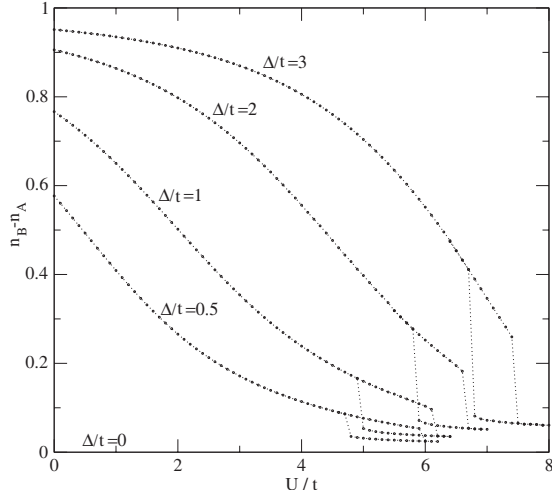


FIG. 5. Staggered charge density $n_B - n_A$ as a function of U for different values of the ionic potential Δ . Our results for $\Delta = 2t$ are in good agreement with those obtained within cluster-DMFT in 2D.⁷

IHM is of the same nature as that found within the single-site DMFT for the one-band Hubbard model.⁹ Finally, we recall that the 2D (Refs. 7 and 8) works reach opposite conclusions regarding the metallic phase of the IHM, indicating a great sensitivity on the procedure used. The metallic phase derived within determinant quantum Monte Carlo⁶ suggests a *quasi-particle peak* at $\omega=0$,⁸ while a *pseudo-gap* like feature is seen in the Lanczos solution of the cluster bath.⁷ Clearly, near the Fermi level our metallic phase is more consistent with the CDMFT calculations. However, the shape of our phase diagram is similar to the one derived in Ref. 6 which indicates that the correct nature of the metallic phase in 2D remains to be investigated.

From the pure Hubbard model it is known that the IPT method is well suited to show the existence of the coexist-

ence region and provides a correct qualitative picture of the metal-insulator transition in infinite dimensions. However, there are some details of this transition, e.g., the precise position or the stability of different phases⁹ which have to be clarified by more sophisticated methods and which are left for further studies.

In summary, we derived the many-body phase diagram of the IHM in the limit of infinite dimensions. For intermediate values of the ionic potential Δ , we find a metallic phase between the BI and the Mott-Hubbard insulating phase which disappears, however, for larger Δ . Our results clearly differ from a previous work which employs the same single-site approach for the IHM.⁵ We believe to have found the correct spectral density in the limit of $U \gg \Delta$. In contrast to Ref. 5, our result in this regime shows clear Mott-Hubbard features, in agreement with the general expectation.⁹ We find first-order phase transitions between the metallic and the MI phases as well as between the band and the Mott insulator. The latter was not reported in previous studies on metal-insulator transitions for the IHM. We show that a discontinuous transition exists already at high dimensions and is not necessarily connected with the bond-order phase as proposed in Ref. 7.

To conclude, the IHM is expected to have a wide range of applicability in correlated (real) materials showing charge order-disorder phase transitions.¹⁸ Therefore, it would be highly interesting to study the stability of the various phases against additional terms in the one-particle Hamiltonian.

R.H. thanks the NATO science division Grant No. CLG 98 1255 for financial support. L.C. acknowledges support from the SFB608 and the Emmy Noether-Programm of the DFG. He also thanks M. S. Laad for discussions as well as the University Paul Cezanne at Marseille for hospitality. G.I.J. acknowledges support from the STCU Grant No. N 3867 and from the Georgian National Science Foundation Grant No. GNSF/ST06/4-018.

¹N. F. Mott, *Metal-Insulator Transitions*, 2nd ed. (Taylor & Francis, London, 1990).

²M. Imada, A. Fujimori, and Y. Tokura, *Rev. Mod. Phys.* **70**, 1039 (1998).

³A. Fuhrmann, D. Heilmann, and H. Monien, *Phys. Rev. B* **73**, 245118 (2006); A. Rosch, *Eur. Phys. J. B* **59**, 495 (2007).

⁴L. Craco, *Phys. Rev. B* **59**, 14837 (1999); L. Craco, *J. Phys.: Condens. Matter* **13**, 263 (2001); see also, Q. Si, M. J. Rozenberg, G. Kotliar, and A. E. Ruckenstein, *Phys. Rev. Lett.* **72**, 2761 (1994).

⁵A. Garg, H. R. Krishnamurthy, and M. Randeria, *Phys. Rev. Lett.* **97**, 046403 (2006).

⁶N. Paris, K. Bouadim, F. Hebert, G. G. Batrouni, and R. T. Scalapart, *Phys. Rev. Lett.* **98**, 046403 (2007).

⁷S. S. Kancharla and E. Dagotto, *Phys. Rev. Lett.* **98**, 016402 (2007).

⁸K. Bouadim, N. Paris, F. Hebert, G. G. Batrouni, and R. T. Scalapart, *Phys. Rev. B* **76**, 085112 (2007).

⁹A. Georges, G. Kotliar, W. Krauth, and M. J. Rozenberg, *Rev. Mod. Phys.* **68**, 13 (1996).

¹⁰M. Fabrizio, A. O. Gogolin, and A. A. Nersesyan, *Phys. Rev. Lett.* **83**, 2014 (1999).

¹¹A. P. Kampf, M. Sekania, G. I. Japaridze, and P. Brune, *J. Phys. C* **15**, 5895 (2003).

¹²G. I. Japaridze, R. Hayn, P. Lombardo, and E. Müller-Hartmann, *Phys. Rev. B* **75**, 245122 (2007).

¹³H. Kajueter and G. Kotliar, *Phys. Rev. Lett.* **77**, 131 (1996).

¹⁴F. Gebhard, E. Jeckelmann, S. Mahler, S. Nishimoto, and R. M. Noack, *Eur. Phys. J. B* **36**, 491 (2003); D. J. García, K. Hallberg, and M. J. Rozenberg, *Phys. Rev. Lett.* **93**, 246403 (2004).

¹⁵M. J. Rozenberg, G. Kotliar, and X. Y. Zhang, *Phys. Rev. B* **49**, 10181 (1994); T. Wegner, M. Potthoff, and W. Nolting, *ibid.* **57**, 6211 (1998).

¹⁶E. Müller-Hartmann, *Z. Phys. B: Condens. Matter* **76**, 211 (1989).

¹⁷D. Tanasković, V. Dobrosavljević, E. Abrahams, and G. Kotliar, *Phys. Rev. Lett.* **91**, 066603 (2003).

¹⁸L. Craco, M. S. Laad, and E. Müller-Hartmann, *Phys. Rev. B* **74**, 064425 (2006).